JACS
JOURNAL OF THE AMERICAN CHEMICAL SOCIETY

ARTICLE

pubs.acs.org/JACS

A Dynamic Covalent, Luminescent Metallopolymer that Undergoes Sol-to-Gel Transition on Temperature Rise

Xavier de Hatten,[†] Nicholas Bell,[‡] Nataliya Yufa,[‡] Gabriel Christmann,[‡] and Jonathan R. Nitschke*[,†]

[†]Department of Chemistry, University of Cambridge, Lensfield Road, Cambridge CB2 1EW, U.K.

[‡]Cavendish Laboratory, University of Cambridge, JJ Thomson Ave, Cambridge CB3 0HE, U.K.

Supporting Information

ABSTRACT: The condensation of linear diamine and dialdehyde subcomponents around copper(I) templates in the presence of bulky trioctylphosphine ancillary ligands gave a linear, conjugated polymeric material in DMSO solution. This polymer solution was observed to undergo sol-to-gel transition as the temperature was raised to 140 °C, in contrast with the behavior of most gel-forming polymers, which do so upon cooling. We attribute the sol-to-gel transition to the formation of $Cu^{I}N_4$ cross-links as the equilibria $2[Cu^{I}N_2P_2] \rightleftarrows [Cu^{I}N_4] + [CuP_n]^+ + (4 - n)P$ favor the right-hand side at higher temperatures. The material was also observed to exhibit thermochromism and photoluminescence, with the color and intensity of both absorption and emission exhibiting temperature dependence. This material thus responds predictably to combinations of stimuli (heat, light, mechanical shear) in an interconnected way, as is required to generate complex function.

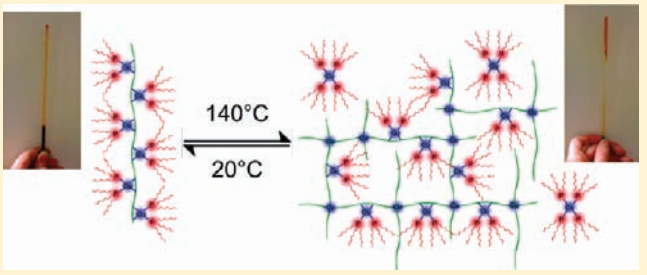

INTRODUCTION

Subcomponent self-assembly,[1] a synthetic technique in which metal templation[2] is used to prepare both dynamic covalent imine (C═N) bonds and coordinative (N→M) linkages during the same overall process, has been employed in the preparation of structures ranging in complexity from helicates[3] to a Borromean link.[4] In recent years it has been used in the preparation of host structures capable of selectively binding guests of technological interest, such as P_4[5] and SF_6.[6] Building on previous reports of the preparation of extended helical structures,[7] here we report the use of subcomponent self-assembly to prepare a linear polymer that is capable of modulated responses to multiple stimuli.

The ability to respond differently to combinations of stimuli can allow for the emergence of complex behavior within a system, as the presence of one stimulus modulates the response to another. Within integrated circuits, for example, an individual transistor's ability to pass current is modulated by a "gate" signal.[8] Neurons likewise aggregate many differently weighted "inputs" into their "output" responses.[9] The formulation of an output based upon two or more inputs constitutes a *logic operation*, and the combination of many logic elements (such as neurons or transistors) allows for computations to occur and complex behavior to emerge. Much interest has fruitfully been paid to logic elements in the context of chemical systems,[10] which has allowed the development of materials capable of complex responses to stimuli[11,12] and ultimately new and useful functions based upon these responses.[13]

Our new polymer is photoluminescent, with the wavelengths and intensities of both absorbances and emissions changing as a function of temperature; the application of one stimulus (thermal) thus alters the material's response to another (light). Its polymer backbone is π-conjugated; the direct linkage of Cu^{I} ions to conjugated polymer backbones has allowed for enhanced electrical conductivity due to orbital overlap in other systems.[14] The polymer is both dynamic covalent[15−19] and metallosupramolecular[12,19,20] in nature, allowing features and functions from both classes of materials to be combined. Perhaps most interesting from a technological point of view, it exhibits the counterintuitive property of undergoing transition from sol to gel as the temperature is raised. Metal ion containing gels[21] have been shown to functionally respond to multiple stimuli[12,22] such as sound,[23] redox potential,[24] magnetism,[25] and light.[26]

RESULTS AND DISCUSSION

As shown in Figure 1, we reasoned that copper(I) templation might serve to knit together linear 1,4-diaminobenzene and 4,4′-diformyl-3,3′-bipyridine subcomponents into polymer **1**, given the demonstrated ability of copper(I) to stabilize imine ligands.[27] Trioctylphosphine (TOP) ligands were introduced in order to cap the vacant coordination sites of the copper ions, taking advantage of the observation that heteroleptic $[CuN_2P_2]^+$ species are favored with respect to homoleptic $[CuN_4]^+$ and $[CuP_4]^+$ complexes.[28−30]

The preparation of **1** thus validated the use of subcomponent self-assembly to make a new class of structurally dynamic conjugated metal-containing polymers.[31] Although the focus of

Received: November 24, 2010
Published: February 15, 2011

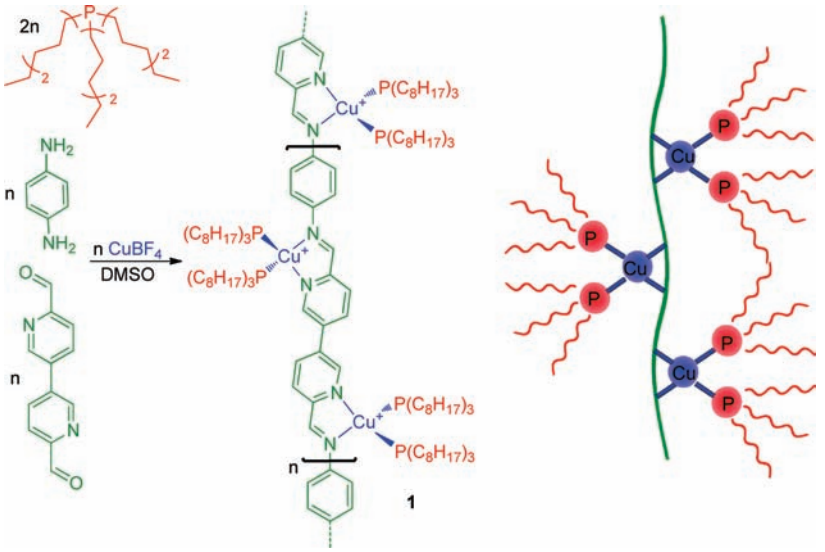

Figure 1. The preparation of conjugated metal−organic polymer **1** from subcomponents (left) and its cartoon representation (right).

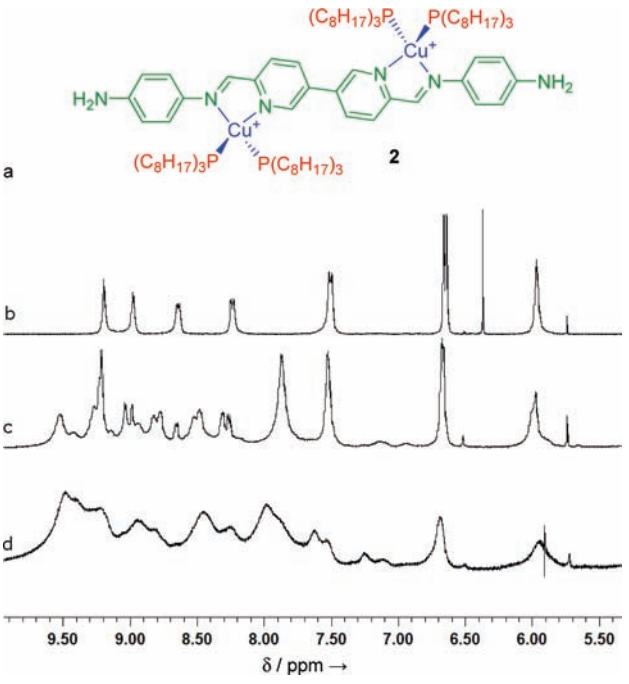

Figure 2. (a) Diagram of the structure of model compound **2** and the aromatic region of ^{1}H NMR spectra in DMSO-d_6 of (b) model compound **2**; (c) a mixture of polymer building blocks (shown in Figure 1) after equilibration in DMSO for 2 days at 80 °C, and (d) the same mixture of building blocks after 12 h at 120 °C and following purification by trituration with dichloromethane.

the present study does not include functions related to the dynamic covalent nature of **1**, such polymers[32] also have been shown to be capable of reconstituting themselves in response to different stimuli, including light,[17] solvent effects,[18] cations,[16] and electrical fields.[33]

Initial attempts to produce polymer **1** involved carrying out the reaction of Figure 1 at 80 °C in DMSO. Although the broadness of the products' ^{1}H NMR signals (Figure 2c) suggested that oligomerization had occurred, the spectrum was consistent with a mixture composed mostly of dicopper complex **2** (Figure 2a) and other short oligomers. In order to increase the size of the chain, the reaction was carried out at 120 °C for 12 h under vacuum in order to remove the water formed during imine condensation and thus to shift the equilibrium toward the formation of imine bonds. After equilibration of the system, the residue was dried at 120 °C under vacuum, and residual low molecular weight compounds were removed by trituration in dichloromethane followed by filtration. The purification step resulted in a mass loss of approximately 30%; we therefore estimate the yield of polymer to be 70%.

The poor solubility of **1** in solvents other than DMSO, its polycationic character, and the relative weakness of the N→Cu coordinative bonds frustrated our attempts to characterize more accurately the material's average molecular weight by gel permeation chromatography (GPC); solution aggregation prevented the use of dynamic light scattering (DLS) for molecular weight determination (as discussed below). MALDI mass spectra likewise gave no information as to the composition of **1** due to its polycationic nature. The synthesis and characterization of model compound **2** (Figure 2a) was thus carried out in order to provide a point of comparison with **1**.

Whereas the ^{1}H NMR spectrum of freshly prepared **1** (Figure 2c) was broad, becoming broader following trituration (Figure 2d), the spectrum of **2** was well-defined (Figure 2b), enabling **2** to be characterized unambiguously by ^{1}H, ^{31}P, NOESY, and COSY NMR and mass spectrometry, in keeping with the observation that heteroleptic $[CuN_2P_2]^+$ species are favored with respect to homoleptic $[CuN_4]^+$ and $[CuP_4]^+$complexes.[28−30]

A mixture of oligomers might be expected to form following mixture of the precursor subcomponents of **2** in a 2:1 diamine: dialdehyde ratio, yet **2** was observed to form cleanly under these conditions. We attribute the selective formation of **2** to two factors: First, the amino groups of 1,4-diaminobenzene are expected to have greater nucleophilicity, as a consequence of

dx.doi.org/10.1021/ja110575s |*J. Am. Chem. Soc.* 2011, 133, 3158–3164

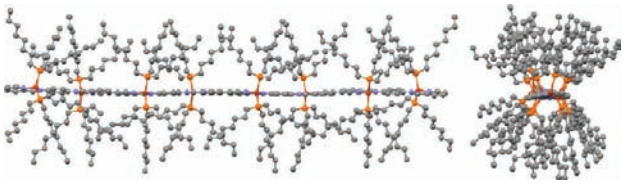

Figure 3. CAChe[36] MM2-minimized structure of an octameric oligomer of **1** viewed facing (left) and down (right) the chain. Carbon is colored in gray, copper is red, nitrogen is blue, and phosphorus is orange. Hydrogen atoms are not shown for clarity.

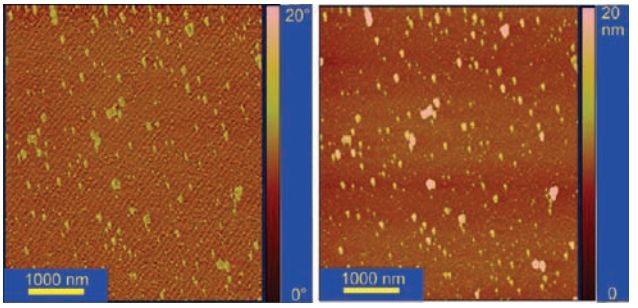

Figure 4. Phase (left) and height (right) AFM microcrographs of aggregated **1** deposited on a SiO_2 surface.

this molecule's more electron-rich character,[34] than the terminal amino groups of **2**, leading longer oligomers to be unstable with respect to **2** in the presence of free 1,4-diaminobenzene. Second, the formation of longer oligomers at the expense of **2** would necessitate the liberation of copper(I). This Cu^I would not be able to attain a coordinatively saturated state[35] with two phosphine and two imine ligands, which has been observed to be a particularly stable coordinative configuration for Cu^I.[28−30]

Upon redissolution of triturated **1** in DMSO, a deep red solution was obtained, the ^{1}H NMR spectrum of which is shown in Figure 2d. For the freshly dichloromethane-triturated sample of **1**, no end-group signals could be distinguished in the ^{1}H NMR spectra (Figure S4, Supporting Information), suggesting that the length of the polymer was greater than 10 monomer units. After 10 cycles of heating to 140 °C and cooling back to room temperature, ^{1}H NMR signals corresponding to $-NH_2$ and $-CHO$ end-groups had become visible. End-group analysis of the ^{1}H NMR spectrum (Figure S5, Supporting Information) allowed estimation of the average length of the degraded polymer to be eight units, corresponding to an average molecular weight M_n = 9.4 kDa and an average length of 65 nm, according to MM2 modeling (Figure 3). Further cycles of heating and cooling resulted in a further decrease in molecular weight, as measured by end-group analysis.

To visualize the structure of **1**, molecular mechanics calculations were performed using the enhanced MM2 force field of CAChe[36] (Figure 3). The energy-minimized structure shows that syndiotacticity allows the TOP ligands to avoid steric clashes. The TOP ligands are best capable of avoiding each other when the aromatic π-system of the polymer chain is planar, facilitating conjugation.

Dynamic light scattering (DLS) and atomic force microscopy (AFM, Figure 4) performed on a triturated sample of **1** (0.7 wt % in DMSO) did not allow molecular weight determination, both techniques revealing the presence of particles of sizes varying from 30 to 900 nm, which suggested that the chains aggregate in solution. We attribute this aggregation to the solvophobic effect of DMSO on the octyl chains, as has been previously observed with other types of amphiphile.[37] These aggregates were not observed for AFM and DLS measurements of **2**, thus highlighting the necessity of having longer polymeric chains for aggregation.

Purified **1** was noted to reversibly form a gel upon heating in DMSO by means of the observation that the solution did not flow upon inversion in a NMR tube (Figure 6), even upon shaking the sample. A concentration of **1** in the range from 2.0 to 0.7 wt % was sufficient to result in the formation of a gel at a temperature between 130 and 140 °C, with higher concentrations being observed to form gels at lower temperatures. Our attempts at carrying out rheology measurements on solutions of **1** were frustrated by the difficulties of taking measurements at 140 °C on a material that is slightly sensitive to degradation in the presence of atmospheric oxygen at room temperature, becoming more sensitive as the temperature increases.

A temperature-cycling ^{1}H NMR experiment (Figure S3, Supporting Information) showed behavior consistent with the formation of a gel as the aromatic signals disappear at high temperature. The sol-to-gel transition is thus demonstrated to be reversible, although some degradation is observed to occur upon cycling: After 10 cycles from 25 to 140 °C, the average size of the polymer, as estimated by ^{1}H NMR end-group analysis, had been reduced from >10 to 8 monomer units, resulting in an approximate 10 °C raising of the gelation temperature. After 15 cycles, the average number of monomer units per oligomer was estimated to be slightly below 8, and sol-to-gel transition was no longer observed. These observations are consistent with the harsh conditions of temperature cycling resulting in a degradation of the polymer chains below the minimal length required to entrap the solvent and to form a gel.

Scanning electron microscopy (SEM) was performed to study the morphology of the xerogel (air-dried gel) formed by the complex. A solution of the complex in DMSO was deposited on a silicon surface and subsequently dried in an oven at 140 °C. The resultant xerogel was examined with no supplementary coating, relying upon the conjugated polymer chain's electron-transport properties. Representative SEM images are shown in Figure 5. A densely entangled three-dimensional network of continuous entwined fibrous nanoassemblies with widths of 100−1000 nm can be seen clearly, characteristic of a desiccated gel.

The sol-to-gel transition of **1** at high temperature is counterintuitive and novel: with few exceptions,[38] sol-to-gel transitions are observed to occur as the temperature is lowered. Neither model compound **2** nor the initial mixture of polymers prior to dichloromethane trituration formed a gel at any temperature up to the boiling point of DMSO, consistent with the necessity of a certain minimal average oligomer length ($n \geq 6$) for the sol-to-gel transition to occur. Although gel formation might be attributed to the aggregation of peripheral octyl chains driven by solvophobic effects,[39] our observations are more consistent with a sol-to-gel transition mechanism involving changes in the coordination environment of the copper(I) centers of **1**.

Our proposed mechanism involves the reversible formation of $[CuN_4]^+$ cross-links between oligomeric **1** chains during sol-to-gel transition (Figure 6). NMR, UV−vis, and photoluminescence data support this mechanism; each is described in turn below. Each $[CuN_4]^+$ cross-link must result from reaction between two $[CuN_2P_2]^+$ units on different chains, with release of one $[Cu(P)_4]^+$ unit into solution. Upon the basis of the observation that complexes of the type $[CuN_2P_2]^+$ do not tend

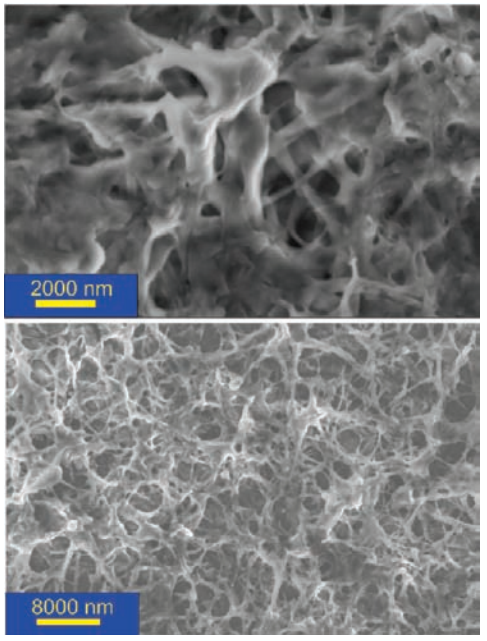

Figure 5. Scanning electron micrographs of the entwined fibrillar network obtained after drying gel **1** at 140 °C on a silicon substrate.

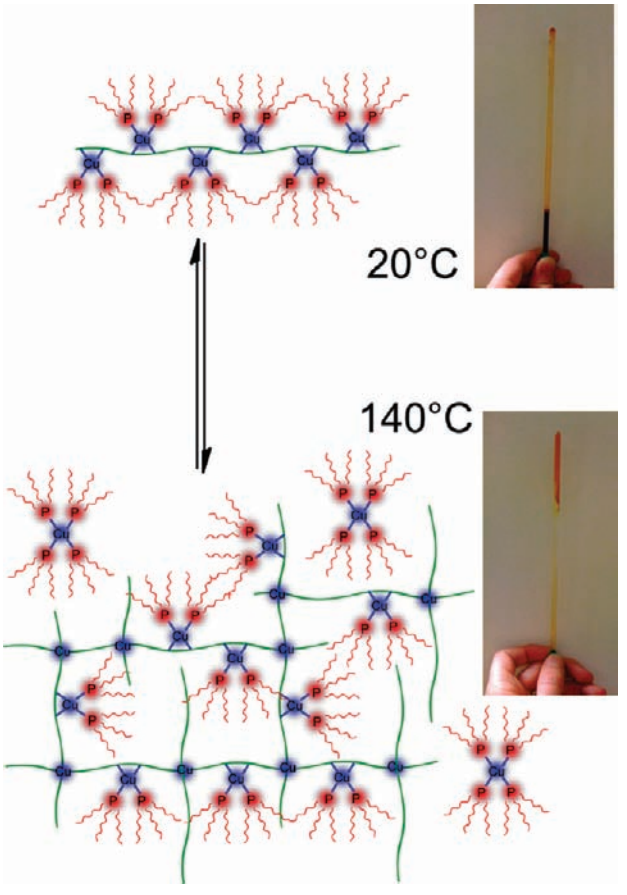

Figure 6. Schematic representation of the gelation mechanism of **1** (left); photographs of inverted NMR tubes showing **1** in solution (top right) and following the sol−gel transition (bottom right).

to undergo ligand exchange to give $[CuN_4]^+$ and $[CuP_4]^+$,[28−30] we conclude that $[CuN_4]^+$ cross-links between oligomeric **1** chains are enthalpically disfavorable but become increasingly favorable due to entropy increase as the temperature is raised, particularly as the equilibria $[CuP_4]^+ \rightleftarrows [CuP_n]^+ + (4 - n)P$ begin to favor the right-hand side at higher temperatures.[28] Such a sol-to-gel transition mechanism is, to the best of our knowledge, unprecedented in the literature, although ligand redistribution reactions in Cu^I complexes are well-known.[28−30]

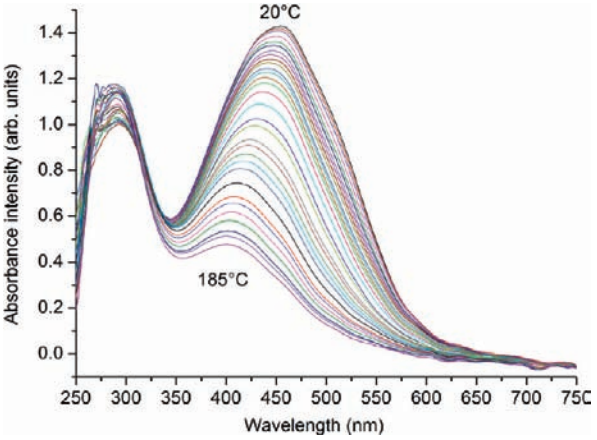

Figure 7. Temperature dependence of the UV−vis absorbance of a DMSO solution of **1**.

The alkyl ^1H and ^{31}P (Figure S6, Supporting Information) NMR spectra of **1** in DMSO that were recorded at 140 °C show signals corresponding to those of $Cu(TOP)_4BF_4$ taken in DMSO at 140 °C. The ^1H NMR peaks corresponding to the backbone of **1** disappear at this temperature (Figure S3, Supporting Information). This observation is consistent with the liberation of free $[Cu(TOP)_4]^+$ during the sol-to-gel transition, as species that are immobilized within the fibrillar network of the gel become NMR-silent.[40]

UV−vis absorption spectra of a solution of **1** in DMSO (0.7 w %) were recorded at temperatures from 20 to 185 °C (Figure 7). At room temperature, two intense bands are observed at 290 and 455 nm, as have been previously observed for related complexes.[30,41] The first band is assigned to an intraligand (IL) $\pi-\pi^*$ transition, and the second one is due to a metal-to-ligand charge transfer (MLCT) involving the imine chelate ligand. Upon heating, the band at 455 nm undergoes a hypochromic shift (decrease in intensity) along with a hypsochromic shift (blue shift) such that at 185 °C the band was observed at 400 nm (Figure 7). The band observed at 290 nm does not change as the temperature was increased, other than decreasing slightly in intensity.

We attribute the slight diminution of the 290 nm band to the sample's slight increase in opacity on heating, related to the formation of the fibrillar network and the subsequent sol-to-gel transition. The hypsochromic shift of the 455 nm band is attributed to the increasing concentration of $[CuN_4]^+$ moieties at the expense of $[CuN_2P_2]^+$; the former absorb at a shorter wavelength than the latter.[28] This band's diminution in intensity is also consistent with decreasing amounts of colored $[CuN_2P_2]^+$ and increasing amounts of colorless $[CuP_n]^+$ as the temperature increases. All of these effects are consistent with our proposed mechanism of gel formation.

The temperature dependence of the photoluminescence of **1** in DMSO was measured on a sample (0.7 wt %) sandwiched between two quartz plates with a path length of ca. 100 μm (Figures 8 and 9). The sample was excited with a continuous

dx.doi.org/10.1021/ja110575s |*J. Am. Chem. Soc.* 2011, 133, 3158–3164

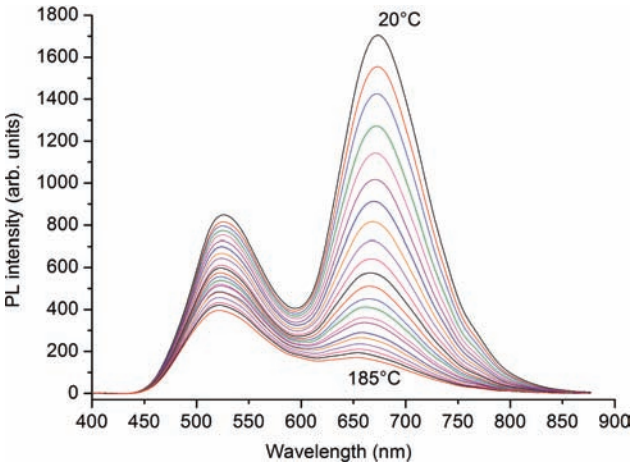

Figure 8. Temperature dependence of the photoluminescence of **1** in DMSO solution recorded between 20 and 185 °C.

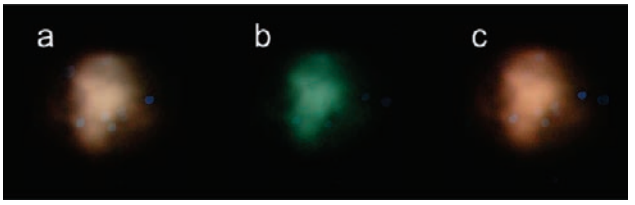

Figure 9. Photoluminescence from the same sample of a DMSO solution of 1 sandwiched between two quartz plates: (a) at 22 °C, (b) heated to 140 °C, and (c) cooled back down to 22 °C. The pale blue dots result from scattering of the excitation laser beam.

laser beam at 600 μW with a spot size of 100 μm for Figure 8 and 2 mm for Figure 9. Both emission bands observed at room temperature, at 525 and 673 nm, can be linked to the absorption bands described above, respectively, the $\pi-\pi^*$ IL and the MLCT bands, with shifts of respectively 235 nm (Stokes shift 1.91 eV) and 218 nm (Stokes shift 0.88 eV). These Stokes shifts are large in comparison with other conjugated polymers.[42] Derivatives of **1** might thus be good candidates for technological applications requiring large Stokes shifts, such as molecular imaging, scintillators, or solar energy conversion. The electroluminescent properties of **1** are currently under investigation.[43]

The comparatively greater diminution of the 673 nm band as the temperature is raised also supports our thesis that the equilibrium between luminescent $[CuN_2P_2]^+$ vs less luminescent $[CuN_4]^+$ and nonluminescent $[CuP_4]^+$ progressively favors the less luminescent side as cross-links form at higher temperatures.

Figure 9 illustrates the tunability of emission intensity and color as a function of temperature. The emission can be seen to change from orange to green when the sample is heated from 20 to 185 °C, returning to orange when the sample is allowed to cool to room temperature.

These data suggest that the structural changes responsible for the gel formation also influence the electronic properties of the polymer, creating a reporting mechanism for the physical state of the material.

The combination of responses to stimuli that **1** expresses, as well as the interactions possible between these responses, could enable **1** and similar materials to be incorporated into devices and systems that are capable of generating complex and useful responses to stimuli. The increase in viscosity that accompanies gel formation permits a thermal signal to be converted into a mechanical response opposite to the response of a typical gel-forming polymer. In addition to *acting*, the gel system can also *report* on its state through thermochromism: an optical measurement will nonintrusively allow for temperature to be determined or monitored. The response of conjugated **1** to current flow could allow for even more complex and useful optoelectronic applications in the domains of electroluminescent materials and photovoltaics; these are currently under investigation.

EXPERIMENTAL SECTION

General. TOP was purchased from TCI Europe and used without further purification; 1,4-phenylenediamine was purchased from Acros Organics and crystallized from hot ethanol before use. Cu-$(CH_3CN)_4BF_4$[44] and 3,3′-bipyridine-6,6′-dicarboxaldehyde[45] were synthesized according to literature protocols. DMSO-d_6 was purchased from Eurisotop and used without further purification. ^{1}H, ^{13}C, and ^{31}P NMR spectra were recorded on a Bruker Avance 500 spectrometer. Chemical shifts are reported in ppm downfield from the residual solvent peak for ^{1}H and the trioctylphosphine oxide signal at 45.0 ppm for ^{31}P.[46] Electronic absorbance spectra were measured in DMSO with a Cary 100 spectrometer. Photoluminescence measurements were recorded on a gel sample (0.7 wt %) sandwiched between two quartz plates with a path length of about 0.1 mm, using a 377 nm laser at 600 μW with a spot size of ca. 100 μm diameter and 20 s accumulation time. The filter cutting wavelength was applied under 450 nm. For both absorbance and photoluminescence spectra, the temperature was allowed to equilibrate for 2−3 min prior to measurement. Dynamic light scattering (DLS) measurements were recorded at 25 °C in DMSO (refractive index n_D = 1.479) on a Malvern Zetasizer Nano Z.

The model of **1** shown in Figure 3 was generated through energy minimization (augmented MM2 force field, 300 cycles) using the CAChe[36] software package. Atomic force microscopy (AFM) measurements were performed on a Dimension 2100 (Veeco Instruments, Santa Barbara, CA) in tapping mode. Phase and height images were taken at speeds of 0.5−1 lines/s using gold-coated silicon tips with spring constants of ∼20−40 N/m. Scanning electron microscopy (SEM) was carried out on a LEO Ultra 55 SEM with a field emission source. Accelerating voltages of 3−5 keV were used. The samples were sufficiently conducting to allow for successful imaging without requiring additional coating.

Preparation of Polymer 1. An oven-dried 10 mL Schlenk flask was charged with 1,4-phenylenediamine (10.8 mg, 0.10 mmol), 3,3′-bipyridine-6,6′-dicarboxaldehyde (21.2 mg, 0.10 mmol), and Cu-$(CH_3CN)_4BF_4$ (62.8 mg, 0.20 mmol) and placed under an inert atmosphere. A solution of trioctylphosphine (148.2 mg, 178.3 mL, 0.40 mmol) in degassed DMSO (1.0 mL) was subsequently added, and the resulting solution was stirred at 120 °C under vacuum until the solvent had evaporated (12 h). The deep red residue was washed four times with 10 mL of distilled DCM. The residue was subsequently dried under dynamic vacuum. The purification step led to a mass loss of 30%; we therefore estimate the yield of purification to be in the range of 70%.

Preparation of the Gel. DMSO-d_6 (0.5 mL) was added to a sample of **1** (5 mg) obtained as described above, and the polymer was dissolved by heating with a heat gun. The solution was subsequently filtered through a cotton plug in a Pasteur pipet to obtain a saturated solution of **1** in DMSO. Material prepared in this way was observed reproducibly to form a gel upon heating that did not flow following inversion of the NMR tube.

Synthesis of Compound 2. Into a Teflon-capped NMR tube were placed 1,4-phenylenediamine (2.27 mg; 0.021 mmol), 3,3′-bipyridine-6,6′-dicarboxaldehyde (2.12 mg, 0.010 mmol), and Cu(CH_3CN)$_4BF_4$ (6.28 mg, 0.020 mmol) under an inert atmosphere. A solution of trioctylphosphine (14.82 mg, 17.83 mL, 0.040 mmol) in degassed DMSO (1.0 mL) was subsequently added. The tube was sealed and the solution was purged of dioxygen by three vacuum/argon fill cycles and left to stand at 80 °C for 12 h. The yield of the reaction is shown to be quantitative. Only peaks derived from the product **2** and dianiline were observed in the NMR and mass spectra, and no signal from the bipyridine is reported. ^{1}H NMR (500 MHz, DMSO-d_6): δ = 9.18 (2H, s), 8.96 (2H, s), 8.63 (2H, d, J = 7.7 Hz), 8.22 (2H, d, J = 7.7 Hz), 7.49 (4H, d, J = 7.8 Hz), 6.63 (4H, d, J = 8.6 Hz), 5.96 (4H, bs), 1.53−1.10 (204H, m). ^{31}P NMR (75 MHz, referenced to residual trioctyl phosphine oxide signal at 46.6 ppm, DMSO-d_6): δ = −20.1 ppm (br, CuN_2P_2). ^{13}C NMR (500 MHz, 300 K DMSO-d_6): δ = 152.5, 151.9, 149.2, 147.5, 136.3, 135.4, 133.5, 127.9, 125.2, 113.9, 31.7, 31.4, 29.113, 29.0, 24.7, 24.2, 22.5, 14.3. ESI-MS: m/z 517.48 ($[M - 4PR_3]^+$), 803.95 ($[Cu_2(PR_3)_4]^{2+}$), 1001.10 ($[M]^{2+}$).

■ ASSOCIATED CONTENT

Supporting Information. Assigned ^{1}H NMR and ESI mass spectra for model compound **2**; NMR spectra, signal assignments, and end-group analysis for **1**. This material is available free of charge via the Internet at http://pubs.acs.org.

■ AUTHOR INFORMATION

Corresponding Author
jrn34@cam.ac.uk

■ ACKNOWLEDGMENT

The authors thank Guillaume Jeanmairet and Yana Hristova, for their help during the early stages of this project, and Prof. Ullrich Steiner, for sharing pertinent insights. Mass spectra were provided by the UK Engineering and Physical Sciences Research Council National MS Service Centre at Swansea. This work was supported by the US Army Research Office and the Marie Curie Intra-European Fellowship Scheme of the 7th EU Framework Program (XdH), and the European Research Council.

■ REFERENCES

(1) Campbell, V. E.; Nitschke, J. R. *Synlett* **2008**, *20*, 2077–3090.
(2) Busch, D. H. *Science* **1971**, *171*, 241–248.
(3) Domer, J.; Slootweg, J. C.; Hupka, F.; Lammertsma, K.; Hahn, F. E. *Angew. Chem., Int. Ed.* **2010**, *49*, 6430–6433.
(4) Chichak, K. S.; Cantrill, S. J.; Pease, A. R.; Chiu, S.-H.; Cave, G. W. V.; Atwood, J. L.; Stoddart, J. F. *Science* **2004**, *304*, 1308–1312.
(5) Mal, P.; Breiner, B.; Rissanen, K.; Nitschke, J. R. *Science* **2009**, *324*, 1697–1699.
(6) Riddell, I. A.; Smulders, M. M. J.; Clegg, J. K.; Nitschke, J. R. *Chem. Commun.* **2011**, *47*, 457–459.
(7) Schultz, D.; Biaso, F.; Shahi, A. R. M.; Geoffroy, M.; Rissanen, K.; Gagliardi, L.; Cramer, C. J.; Nitschke, J. R. *Chem.—Eur. J.* **2008**, *14*, 7180–7185. Dai, Y.; Katz, T. J.; Nichols, D. A. *Angew. Chem., Int. Ed. Engl.* **1996**, *35*, 2109–2111.
(8) Horowitz, P.; Hill, W. *The Art of Electronics*, 2nd ed.; Cambridge University Press: Cambridge (UK), 1989.
(9) Levitan, I. B.; Kaczmarek, L. K. *The Neuron: Cell and Molecular Biology*, 3rd ed.; Oxford University Press: Oxford, 2002.
(10) Allen, V. C.; Robertson, C. C.; Turega, S. M.; Philp, D. *Org. Lett.* **2010**, *12*, 1920–1923. de Silva, A. P.; McClenaghan, N. D. *Chem.—Eur. J.* **2004**, *10*, 574–586.
(11) Appel, E. A.; Biedermann, F.; Rauwald, U.; Jones, S. T.; Zayed, J. M.; Scherman, O. A. *J. Am. Chem. Soc.* **2010**, *132*, 14251–14260. Gupta, T.; van der Boom Milko, E. *Angew. Chem., Int. Ed.* **2008**, *47*, 5322–6. Dadon, Z.; Wagner, N.; Ashkenasy, G. *Angew. Chem., Int. Ed.* **2008**, *47*, 6128–6136. Liu, Y.; Yu, Y.; Gao, J.; Wang, Z.; Zhang, X. *Angew. Chem., Int. Ed.* **2010**, *49*, 6576–6579.
(12) Beck, J. B.; Rowan, S. J. *J. Am. Chem. Soc.* **2003**, *125*, 13922–13923.
(13) Yoon, H. J.; Kuwabara, J.; Kim, J. H.; Mirkin, C. A. *Science* **2010**, *330*, 66–69; Spokoyny, A. M.; Li, T. C.; Farha, O. K.; Machan, C. W.; She, C.; Stern, C. L.; Marks, T. J.; Hupp, J. T.; Mirkin, C. A. *Angew. Chem., Int. Ed.* **2010**, *49*, 5339–5343; S5339/1–S5339/50. Balzani, V.; Credi, A.; Raymo, F. M.; Stoddart, J. F. *Angew. Chem., Int. Ed.* **2000**, *39*, 3348. Sorde, N.; Das, G.; Matile, S. *Proc. Natl. Acad. Sci. U.S.A.* **2003**, *100*, 11964–11969. Peng, H.; Sun, X.; Cai, F.; Chen, X.; Zhu, Y.; Liao, G.; Chen, D.; Li, Q.; Lu, Y.; Zhu, Y.; Jia, Q. *Nat. Nano.* **2009**, *4*, 738–741. Motiei, L.; Lahav, M.; Freeman, D.; van der Boom, M. E. *J. Am. Chem. Soc.* **2009**, *131*, 3468–3469. Yasuda, T.; Tanabe, K.; Tsuji, T.; Coti, K. K.; Aprahamian, I.; Stoddart, J. F.; Kato, T. *Chem. Commun.* **2010**, *46*, 1224–1226.
(14) Holliday, B. J.; Swager, T. M. *Chem. Commun.* **2005**, 23–36.
(15) Rowan, S. J.; Cantrill, S. J.; Cousins, G. R. L.; Sanders, J. K. M.; Stoddart, J. F. *Angew. Chem., Int. Ed.* **2002**, *41*, 899–952. Jackson, A. W.; Fulton, D. A. *Chem. Commun.* **2010**, *46*, 6051–6053. Skene, W. G.; Lehn, J.-M. P. *Proc. Natl. Acad. Sci. U.S.A.* **2004**, *101*, 8270–8275. Kamplain, J. W.; Bielawski, C. W. *Chem. Commun.* **2006**, 1727–1729. Amamoto, Y.; Higaki, Y.; Matsuda, Y.; Otsuka, H.; Takahara, A. *J. Am. Chem. Soc.* **2007**, *129*, 13298–13304. Amamoto, Y.; Kikuchi, M.; Otsuka, H.; Takahara, A. *Macromolecules* **2010**, *43*, 5470–5473.
(16) Giuseppone, N.; Fuks, G.; Lehn, J.-M. *Chem.—Eur. J.* **2006**, *12*, 1723–1735.
(17) Otsuka, H.; Nagano, S.; Kobashi, Y.; Maeda, T.; Takahara, A. *Chem. Commun.* **2010**, *46*, 1150–1152.
(18) Folmer-Andersen, J. F.; Lehn, J.-M. *Angew. Chem., Int. Ed.* **2009**, *48*, 7664–7667; S7664/1–S7664/9.
(19) Buey, J.; Swager, T. M. *Angew. Chem., Int. Ed.* **2000**, *39*, 608–612.
(20) Richardson, C.; Steel, P. J. *Eur. J. Inorg. Chem.* **2003**, 405–408. Dobrawa, R.; Wurthner, F. *J. Polym. Sci., Part A: Polym. Chem.* **2005**, *43*, 4981–4995. Ikeda, M.; Tanaka, Y.; Hasegawa, T.; Furusho, Y.; Yashima, E. *J. Am. Chem. Soc.* **2006**, *128*, 6806–6807.
(21) Piepenbrock, M.-O. M.; Lloyd, G. O.; Clarke, N.; Steed, J. W. *Chem. Rev.* **2010**, *110*, 1960–2004. Fages, F. *Angew. Chem., Int. Ed.* **2006**, *45*, 1680–1682. Weng, W.; Beck, J. B.; Jamieson, A. M.; Rowan, S. J. *J. Am. Chem. Soc.* **2006**, *128*, 11663–11672.
(22) Kim, H.-J.; Lee, J.-H.; Lee, M. *Angew. Chem., Int. Ed.* **2005**, *44*, 5810–5814. Liu, J.; He, P.; Yan, J.; Fang, X.; Peng, J.; Liu, K.; Fang, Y. *Adv. Mater.* **2008**, *20*, 2508–2511.
(23) Kotal, A.; Paira, T. K.; Banerjee, S.; Mandal, T. K. *Langmuir* **2009**, *26*, 6576–6582.
(24) Kawano, S.; Fujita, N.; Shinkai, S. *J. Am. Chem. Soc.* **2004**, *126*, 8592–8593. Peng, F.; Li, G.; Liu, X.; Wu, S.; Tong, Z. *J. Am. Chem. Soc.* **2008**, *130*, 16166–16167.
(25) Grondin, P.; Roubeau, O.; Castro, M.; Saadaoui, H.; Colin, A.; Clérac, R. *Langmuir* **2010**, *26*, 5184–5195. Roubeau, O.; Colin, A.; Schmitt, V.; Clerac, R. *Angew. Chem., Int. Ed.* **2004**, *43*, 3283–3286.
(26) Lam, S.-T.; Wang, G.; Yam, V. W.-W. *Organometallics* **2008**, *27*, 4545–4548. Tam, A. Y.-Y.; Wong, K. M.-C.; Zhu, N.; Wang, G.; Yam, V. W.-W. *Langmuir* **2009**, *25*, 8685–8695. Shirakawa, M.; Fujita, N.; Tani, T.; Kaneko, K.; Ojima, M.; Fujii, A.; Ozaki, M.; Shinkai, S. *Chem.—Eur. J.* **2007**, *13*, 4155–4162.
(27) Nitschke, J. R. *Angew. Chem., Int. Ed.* **2004**, *43*, 3073–3075.
(28) Engelhardt, L. M.; Pakawatchai, C.; White, A. H.; Healy, P. C. *J. Chem. Soc., Dalton Trans.* **1985**, 125–33.
(29) Nohra, B.; Lescop, C.; Hissler, M.; Reau, R. *Phosphorus, Sulfur Silicon Relat. Elem.* **2008**, *183*, 253–257. Oliveri, C. G.; Gianneschi, N. C.; Nguyen, S. T.; Mirkin, C. A.; Stern, C. L.; Wawrzak, Z.; Pink, M. *J. Am. Chem. Soc.* **2006**, *128*, 16286–16296.

(30) Zhang, Q.; Ding, J.; Cheng, Y.; Wang, L.; Xie, Z.; Jing, X.; Wang, F. *Adv. Funct. Mater.* **2007**, *17*, 2983–2990.
(31) Tennyson, A. G.; Norris, B.; Bielawski, C. W. *Macromolecules* **2010**, *43*, 6923–6935.
(32) Maeda, T.; Otsuka, H.; Takahara, A. *Prog. Polym. Sci.* **2009**, *34*, 581–604.
(33) Giuseppone, N.; Lehn, J.-M. *Angew. Chem., Int. Ed.* **2006**, *45*, 4619–4624.
(34) Schultz, D.; Nitschke, J. R. *J. Am. Chem. Soc.* **2006**, *128*, 9887–9892.
(35) De, S.; Mahata, K.; Schmittel, M. *Chem. Soc. Rev.* **2010**, *39*, 1555–1575. Schultz, D.; Nitschke, J. R. *Proc. Natl. Acad. Sci. U.S.A.* **2005**, *102*, 11191–11195.
(36) *CAChe WorkSystem v. 6.1.12.33*; Fujitsu Limited, 2007.
(37) Mohmeyer, N.; Schmidt, H.-W. *Chem.—Eur. J.* **2007**, *13*, 4499–4509. Seo, S.; Park, J.; Chang, J. *Langmuir* **2009**, *25*, 8439–8441.
(38) Jeong, Y.; Joo, M. K.; Sohn, Y. S.; Jeong, B. *Adv. Mater.* **2007**, *19*, 3947–3950. Kuroiwa, K.; Shibata, T.; Takada, A.; Nemoto, N.; Kimizuka, N. *J. Am. Chem. Soc.* **2004**, *126*, 2016–2021.
(39) John, G.; Jung, J. H.; Masuda, M.; Shimizu, T. *Langmuir* **2004**, *20*, 2060–2065. Wojtyk, J.; McKerrow, A.; Kazmaier, P.; Buncel, E. *Can. J. Chem.* **1999**, *77*, 903–912.
(40) Smith, D. K. *Chem. Soc. Rev.* **2009**, *38*, 684–694.
(41) McCormick, T.; Jia, W.-L.; Wang, S. *Inorg. Chem.* **2006**, *45*, 147–55. Jia, W. L.; McCormick, T.; Tao, Y.; Lu, J.-P.; Wang, S. *Inorg. Chem.* **2005**, *44*, 5706–5712.
(42) Dutta, T.; Woody, K. B.; Parkin, S. R.; Watson, M. D.; Gierschner, J. *J. Am. Chem. Soc.* **2009**, *131*, 17321–17327.
(43) Kraft, A.; Grimsdale, A. C.; Holmes, A. B. *Angew. Chem., Int. Ed.* **1998**, *37*, 403–428.
(44) Ogura, T. *Transition Met. Chem.* **1976**, *1*, 179–82.
(45) Attias, A.-J.; Cavalli, C.; Bloch, B.; Guillou, N.; Noeel, C. *Chem. Mater.* **1999**, *11*, 2057–2068.
(46) Hens, Z.; Moreels, I.; Martins, J. C. *ChemPhysChem* **2005**, *6*, 2578–2584.